AFBMD-
ASTIA Document No.

Copy No. 13 of 137 copies, Series A

"ACADEMY OF SCIENCES, USSR (MOSCOW)

"FLOW PAST A CIRCULAR CYLINDER WITH A

"DETACHED SHOCK WAVE

[Prepared by]

"O. M. Belotserkovskii"

[From: Vychislitel'naia Matematika (3), 149-185 (1958)]

Translated by
G. Adashko

Edited by
M. Holt

RESEARCH AND ADVANCED DEVELOPMENT DIVISION
AVCO CORPORATION
Wilmington, Massachusetts

Project WS 107A-2

TECHNICAL MEMORANDUM

RAD-9-TM-59-66

Contract Number AF04(647)-305

30 September 1959

APPROVED

F. W. Diederich
Chief, Aerodynamics Section
Engineering Department

A. Kahane
Manager
Engineering Department

Prepared for

AIR FORCE BALLISTIC MISSILE DIVISION
AIR RESEARCH AND DEVELOPMENT COMMAND
UNITED STATES AIR FORCE
Air Force Unit Post Office
Los Angeles 45, California

ABSTRACT

The general method of Dorodnitsyn (14), for integrating first-order partial differential equations of mixed type, is applied to calculate the flow of a uniform supersonic or hypersonic stream past a circular cylinder. Using polar coordinates referred to the center of the cylinder, the equations of motions are reduced to an approximating system of ordinary differential equations in the angular coordinate, by prescribing the variation of key dependent variables with radial distance. In the first approximation this variation is linear, in the second approximation it is quadratic and so on. The boundary conditions applied to the ordinary differential equations are given by symmetry conditions and conditions that certain equations pass smoothly through singularities near the sonic line.

Flow of a perfect gas past a circular cylinder is calculated for free-stream Mach numbers of 2.13, 2.5, and 4.0 using the first and second approximations, and for free-stream Mach numbers of 3.0 and 5.0 using the first, second, and third approximations.

Results show excellent agreement with experimental data. The method can be extended to calculate the flow of a nonperfect gas past cylinders or bodies of revolution of general shape.

ILLUSTRATIONS

ILLUSTRATIONS (Cont'd)

Figure 8 Pressure on the shock wave at various approximations for $M_\infty = 3.0$

------ N = 1; ——— N = 2; ΔΔΔ N = 3

9 Shock wave and sonic line in various approximations at $M_\infty = 3.0$

------ N = 1; ——— N = 2; ΔΔΔ N = 3

10 Shock wave and sonic line in various approximations for $M_\infty = 5.0$

------ N = 1; ——— N = 2; ΔΔΔ N = 3

11 Distance from the surface of the cylinder to the shock wave, determined by calculation and experimentally

Experiment: Kim, Alperin ○ ○ ○;

Calculation: Tamada —·—·—, Hida ----------, Smurov x x x;

Method of integral relations (N = 2 or 3) ▲ ▲ ▲

12 Comparison of the distribution of the pressure along the surface of the cylinder (N = 2) with experiment at $M_\infty = 2.5$

——— N = 2; ● ● ● experiment

13 Comparison of the distribution of the pressure along the surface of the cylinder (N=1,2,3) with experiment $M_\infty = 3.0$

------ N = 1; ——— N = 2; ΔΔΔ N = 3;

○ ○ ○ experiment

14 Comparison of the distribution of pressure along the surface of a cylinder (N=2) with experiment $M_\infty = 4.0$

——— N = 2; ● ● ● experiment

ILLUSTRATIONS (Cont'd)

TABLES

SYMBOLS USED

x, y	rectangular coordinates
r, θ	polar coordinates (θ is measured from the stagnation point)
M	Mach number
w, p, ρ	dimensionless values of the velocity, pressure, and density
w_x, w_y	components of the velocity w in x and y directions
u, v	components of the velocity w in r and θ directions
$c = \sqrt{\frac{\gamma-1}{2}(1-w^2)}$	dimensionless velocity of sound
$\phi = p/\rho^\gamma$	vorticity function
ψ	stream function
γ	adiabatic exponent
$k = \frac{\gamma-1}{2\gamma}$	
σ	inclination of the shock wave to the direction of the incident stream
$\epsilon(\theta)$	distance from the surface of the body to the shock wave along θ = const [$\epsilon_0 = \epsilon(\theta)$]
$t = rv$	
$r = (1-w^2)^{1/(\gamma-1)}$	
$s = \rho uv$	
$g = kp + \rho v^2$	

SYMBOLS USED (Cont'd)

$H = kp + \rho u^2$

$h = ru$.

Subscripts:

∞	values ahead of the shock wave
i	values on the shock wave
$i = 2, 3, \ldots, N$	values on the intermediate lines behind the shock wave
0	values on the surface of the body.

INTRODUCTION

Although the problem of flow past a body with a detached shock wave has been investigated by many authors, most of them only considered an approximate statement of the problem. The difficulty in problems of this type is that the gas flow is of mixed type, where on one side of the transition (sonic) line the motion is subsonic (elliptic system of equations), while on the other side the speed is supersonic (hyperbolic system of equations). The velocity varies over a rather wide range, from zero (at the stagnation point) to supersonic, and ordinary linearization methods fail. In addition, the boundary conditions of the problem are specified both on the body and on the shock wave, but the shape and position of the latter are not known is advance.

In many papers, the solution of this problem is given in series form. Thus, G.S. Smurov (1) in an analysis of the flow of a supersonic stream of gas past a circular cylinder writes the stream function in the vicinity of the symmetry axis in the form of a series, coefficients of which are determined from the boundary conditions of the problem. Smurov finds the distance ϵ_0 from the surface of the body to the shock wave along the axis of symmetry, and also the pressure distribution on the body near the stagnation point. His calculated data are presented in Fig. 11, and it is seen that they differ considerably from experimental results. It must be noted that Smurov's paper is one of the first in this field. I.A. Panichkin (2) and H. Melkus (3) expand the velocity along the axis of symmetry in a series and, assuming the shock wave to be in the form of a hyperbola, find the ratio $\frac{\epsilon_0}{R_0}$ for various values of the incident stream Mach number M_∞ (ϵ_0 is the radius of curvature of the wave at its crest). C.C. Lin and S.I. Rubinov (4), also using a series expansion, obtain a relation between the position of the shock wave and the radius of curvature of the body at the nose. The method of series expansion makes it possible to investigate only a small region of the flow in the vicinity of the axis of symmetry or else in the vicinity of the stagnation point of the body, and since there is no information on the region of convergence of these series, attempts by several authors to extend these solutions to the sonic line must be deemed unsuccessful.

The possibility of obtaining an analytic solution behind a curved shock wave in the hodograph plane has also been investigated. G. Guderley (5) and A. Busemann (6) considered the case when the Mach number of the incident stream is close to unity. This enabled them to assume the flow behind the wave to be isentropic, and so to use the Chaplygin differential equations. K. Hida (7), using two particular solutions of Tricomi's equation, obtains formulas to estimate the asymptotic position of the detached shock wave for flow of a gas with M_∞ close to unity past blunt-nosed bodies.

September 1959

The flow in the vicinity of the crest of the wave is considered by Hida to be isentropic. He considers this flow in the hodograph plane and neglects the influence of the streamline corresponding to the surface of the body, in view of the closeness of M_∞ to unity. However in the general case, one cannot neglect the influence of the vorticity behind the detached shock wave. It is difficult to obtain an analytic solution for rotational flow in the hodograph plane because it is difficult to write down the boundary conditions along the surface of the body, and also to transform these streams into the hodograph plane.

K. Tamada (8) and K. Hida (9) found the position and shape of the shock wave for flow around a sphere and a circular cylinder by assuming that the wave is followed by rotational flow of an incompressible liquid. T. Kawamura (10) expands in this case all the hydrodynamic variables in a series in the vicinity of the stagnation point and, assuming a hyperbolic or a parabolic shape of shock wave, he determines the distance from the wave to the surface of the cylinder or sphere. The results obtained by these authors are in fair agreement with experiment for flow around a sphere, but the agreement is much worse for flow around a circular cylinder, as can be seen from Fig. 11. S. Uchida and M. Yasuhara (11) propose an approximate graphical method for calculating the flow behind a curved shock wave, in which they must first specify the complete flow pattern. The boundary conditions on the wave are satisfied approximately, and the accuracy of the method diminishes rapidly on approaching the sonic line. The distance ϵ_0 from the body to the wave, obtained by the authors at $M_\infty = 2.0$, is in good agreement with experiment.

Another way of obtaining an approximate solution was proposed by J. W. Maccoll and J. Codd (12) and by A. R. Mitchell (13); specifying the experimentally obtained shape and position of a shock wave, they used the relaxation method to calculate the flow around a body with a flat nose. J. W. Maccoll and J. Codd considered the flow behind the wave to be free of vorticity ($M_\infty = 1.5$).

The use of electronic computers makes it possible to obtain complete results of any required accuracy for the problem in its rigorous form. A sufficiently effective method for use with electronic computers is one in which integration of the system of nonlinear partial difference equations is reduced to a numerical solution of a certain approximating system of ordinary differential equations. This method was proposed by Academician A. A. Dorodnitsyn, and was reported together with certain results of the calculations at the Third All-Union Mathematical Congress (14).

In another paper (15), we used this method to obtain a solution of the problem of the flow past a plane body of arbitrary shape with an axis of symmetry and a detached shock wave. In the present paper, we give the formulas and results for a circular cylinder.

All the calculations were made on the BESM high-speed electronic computer of the USSR Academy of Sciences, built at the Institute for Precision Mechanics and Computational Engineering under the leadership of Academician S. A. Lebedev.

I express my deep gratitude to Comrades E. S. Bogomolova, N. S. Malinina, V. P. Blasova, N. V. Mel'tsis, A. I. Bykova, L. V. Papandina, A. N. Belova, and others who helped in checking the formulas, in the performance of the preliminary calculations, and also in the processing of the data obtained.

I. STATEMENT OF THE PROBLEM

Let a plane-parallel supersonic stream ($M_\infty > 1$) of an ideal gas be incident with constant velocity w_∞ on a circular cylinder. A shock wave, the shape and position of which are unknown beforehand, is produced in front of the cylinder. It is required to calculate the mixed rotational flow of the compressed gas in the region bounded by the shock wave, the axis of symmetry, the surface of the body, and the first limiting characteristic (or characteristics) passing between the wave and the body and bounding the minimum region of influence. Outside this region, the calculation of the flow can be made, say, by the method of characteristics.

We introduce dimensionless quantities which relate the velocity to the maximum velocity, the pressure and density to the stagnation pressure and density ahead of the shock wave, and linear dimensions to the radius of the cylinder. The equations of motion, continuity, and energy (adiabatic condition) then become, in vector form

$$\left.\begin{aligned} &\operatorname{curl}\vec{w}\times\vec{w}+\frac{\nabla w^2}{2}+\frac{\nabla(kp)}{\rho}=0\\ &\nabla(\rho\vec{w})=0\\ &\vec{w}\nabla\frac{p}{\rho^{\gamma}}=0 \end{aligned}\right\} \qquad (1.1)$$

where w, p, and ρ are the velocity, pressure, and density behind the shock wave, and γ is the adiabatic exponent,

$$k=\frac{\gamma-1}{2\gamma}$$

(for air $\gamma = 1.40$ and $k = 1/7$).

The dimensionless form of the Bernoulli integral is

$$w^2+\frac{p}{\rho}=1\,. \qquad (1.2)$$

The equation of continuity leads to the conclusion that there exists a stream function $\psi(r,\theta)$ such that

$$\frac{d\psi}{dr}=\rho v,\ \frac{\partial\psi}{\partial\theta}=-r\rho u \qquad (1.3)$$

hence

$$\frac{\partial \psi}{\partial \theta} = \rho \left(v \frac{dr}{d\theta} - ru \right) . \tag{1.4}$$

If we introduce a vorticity function $\phi = p/\rho^{\gamma}$ (entropy $S = C_v \ln \phi$), we obtain from the adiabatic condition and from (1.3)

$$\phi \equiv \frac{p}{\rho^{\gamma}} = \phi(\psi) \tag{1.5}$$

after which, taking (1.2) into account, we find

$$p = \rho(1 - w^2) = r^{\gamma} \cdot \phi^{-\frac{1}{\gamma - 1}} \tag{1.6}$$

$$\rho = r\phi^{-\frac{1}{\gamma - 1}} \tag{1.7}$$

where

$$r = (1 - w^2)^{\frac{1}{\gamma - 1}} . \tag{1.8}$$

The velocity of sound is defined as follows:

$$c^2 = \gamma \frac{kp}{\rho} = \frac{\gamma - 1}{2} (1 - w^2) . \tag{1.9}$$

We rewrite the system (1.1) in polar coordinates r, θ (Fig. 1), and introduce the Bernoulli integral in place of one of the equations of motion. We then obtain a system equivalent to (1.1). Together with Eq. (1.4), the new system will be

$$\left.\begin{aligned} &\frac{\partial rH}{\partial r} + \frac{\partial s}{\partial \theta} = g \\ &\frac{\partial rH}{\partial r} + \frac{\partial t}{\partial \theta} = 0 \\ &\phi \equiv \frac{p}{\rho^{\gamma}} = \phi(\psi) \\ &\frac{d\psi}{d\theta} = \rho \left(v \frac{dr}{d\theta} - ru \right) . \end{aligned}\right\} \tag{1.10}$$

Here $H = kp + \rho u^2$, $s = \rho uv$, $g = kp + \rho v^2$, $h = ru$, $t = rv$, and p, ρ, r are found from (1.6) -- (1.8). The unknown functions in this system are u, v, ψ, and ϕ.

We now write down the boundary conditions of the problem. On the surface of the cylinder ($r = r_0 = 1$) we have

$$u = 0, \psi = 0, \phi = \frac{4\gamma}{\gamma^2 - 1} \left(\frac{\gamma - 1}{\gamma + 1} \right)^{\gamma} \frac{1}{w_\infty^{2\gamma}} \left[\frac{w_\infty^2}{1 - w_\infty^2} - \frac{(\gamma - 1)^2}{4\gamma} \right] = \text{const.} \tag{1.11}$$

We write the equation of the wave in the following form

$$r(\theta) = 1 + \epsilon(\theta) \tag{A1}$$

where $\epsilon(\theta)$ is the distance from the surface of the body to the wave along the ray θ = const. The relations for the tangential and normal components of the velocity on the shock wave are, according to Sauer (16),

$$w_t = w_{t\infty}$$

$$w_n w_{n\infty} = \frac{\gamma - 1}{\gamma + 1} (1 - w_t^2) \ . \tag{A2}$$

Furthermore

$$w_{t\infty} = w_\infty \cos \sigma, \ w_{n\infty} = w_\infty \sin \sigma \ ,$$

$$\tan \sigma = \frac{w_\infty - w_x}{w_y} \text{ and } w_n = w_{n\infty} - \frac{w_y}{\cos \sigma} \tag{A3}$$

where σ is the angle of inclination of the wave to the direction of the incident stream, and the index ∞ denotes values ahead of the shock wave.

Hence

$$\left.\begin{aligned} w_y &= \frac{w_\infty}{\gamma + 1} \sin 2\sigma \left(1 - \frac{1}{M_\infty^2 \sin^2 \sigma} \right) \\ w_x &= w_\infty \left[1 - \frac{2}{\gamma + 1} \sin^2 \sigma \left(1 - \frac{1}{M_\infty^2 \sin^2 \sigma} \right) \right] . \end{aligned}\right\} \tag{1.12}$$

The necessary conditions for the velocities are then written

$$\left.\begin{aligned} u &= w_y \sin \theta - w_x \cos \theta \\ v &= w_x \sin \theta + w_y \cos \theta \ . \end{aligned}\right\} \tag{1.13}$$

From the pressure and density relations on the wave

$$p = \frac{4\gamma}{\gamma^2 - 1} (1 - w_\infty^2)^{\frac{\gamma}{\gamma - 1}} \left[\frac{w_\infty^2 \sin^2 \sigma}{1 - w_\infty^2} - \frac{(\gamma - 1)^2}{4\gamma} \right]$$

$$\rho = \frac{\gamma + 1}{\gamma - 1} (1 - w_\infty^2)^{\frac{1}{\gamma - 1}} \frac{w_\infty^2}{1 + (1 - w_\infty^2) \cot^2 \sigma} \qquad A4$$

we obtain the boundary condition for $\phi = p/\rho^\gamma$:

$$\phi = \frac{4\gamma}{\gamma^2 - 1} \left(\frac{\gamma - 1}{\gamma + 1} \right)^\gamma \left[\omega - \frac{(\gamma - 1)^2}{4\gamma} \right] \left(1 + \frac{1}{\omega} \right)^\gamma \qquad (1.14)$$

where

$$\omega = \frac{w_\infty^2 \sin^2 \sigma}{1 - w_\infty^2} . \qquad A5$$

Now the stream function has no discontinuity along the wave, and consequently,

$$\psi = \psi_\infty = w_\infty (1 - w_\infty^2)^{\frac{1}{\gamma - 1}} (1 + \epsilon) \sin \theta \ . \qquad (1.15)$$

From the obvious geometric relationship on the wave ($dy/dx = \tan \sigma$) we obtain an equation for $\epsilon(\theta)$:

$$\frac{d\epsilon}{d\theta} = - (1 + \epsilon) \cot (\sigma + \theta) \ . \qquad (1.16)$$

II. METHOD OF SOLUTION

As already noted in the introduction, the problem posed is solved by the method of integral relations (14).

We set up an approximating system for the system of equations (1.10). For this purpose, we draw between the body and the wave a set of N-1 lines that are equidistant along r :

$$r = r_i(\theta) = 1 + \xi_i \epsilon(\theta), \quad \left(\xi_i = \frac{N - i + 1}{N}\right). \qquad \text{B1}$$

These lines break up the region of integration into N strips (see Fig. 1). We denote all the quantities on the i^{th} intermediate line by the index i , on the shock wave ($i = 1$) by the index 1, and on the surface of the body by the index 0.

By integrating the first two equations of (1.10) along an arbitrary ray θ = const from the surface of the body, $r = 1$, to the boundary of each of the strips, we obtain 2N independent integral equations

$$\frac{d}{d\theta}\int_1^{r_i} s(r,\theta)\,dr - s_i\xi_i\frac{d\epsilon}{d\theta} + r_i H_i - H_0 = \int_1^{r_i} g(r,\theta)\,dr \qquad (2.1)$$

$$\frac{d}{d\theta}\int_1^{r_i} \varepsilon(r,\theta)\,dr - \varepsilon_i\xi_i\frac{d\epsilon}{d\theta} + r_i h_i - h_0 = 0$$

$$(i = 1,2,\ldots,N)\,. \qquad (2.2)$$

We now approximate any integrand $f(r,\theta)$ by means of an interpolation polynomial of degree N in r , taking the interpolation points to be the boundaries of the strips

$$f(r,\theta) = \sum_{m=0}^{N} a_m(\theta)\left[\frac{r-1}{\epsilon(\theta)}\right]^m \qquad (2.3)$$

where the coefficients $a_m(\theta)$ depend linearly on the values of the corresponding functions on the boundaries of the strips.

Next, writing down the two last equations of (1.10) along each of the N-1 intermediate lines, $r = r_i(\theta)$ (ψ and ϕ on the wave and on the body are determined from the boundary conditions), and taking Eq. (1.16) into account, we obtain

an approximating system consisting of $4N-1$ equations for the unknowns ϵ, σ, v_0, u_i, v_i, ψ_i, ϕ_i ($i = 2, 3, \ldots, N$). In normal form, this system can be written schematically as:

$$\frac{d\epsilon}{d\theta} = -(1+\epsilon)\cot(\sigma+\theta)$$

$$\frac{d\sigma}{d\theta} = F$$

$$\frac{dv_0}{d\theta} = \frac{E_0}{\frac{\gamma-1}{\gamma+1} - w_0^2}$$

$$\frac{d\psi_i}{d\theta} = \rho_i \left[\frac{dr_i}{d\theta} v_i - r_i u_i\right]$$

$$\frac{du_i}{d\theta} = \frac{1}{t_i \phi_i^{-\frac{1}{\gamma-1}}} \left[s_i - u_i \phi_i^{-\frac{1}{\gamma-1}} \cdot t_i' + \frac{s_i}{\gamma-1} \frac{d \ln \phi_i}{d\psi_i} \frac{d\psi_i}{d\theta}\right]$$

$$\frac{dv_i}{d\theta} = \frac{E_i}{\frac{\gamma-1+2u_i^2}{\gamma+1} - w_i^2}$$

$$\phi_i = \phi_{i*}(\psi_i)$$

$$i = 2, 3, \ldots, N \quad . \tag{2.4}$$

Here

$$F = \frac{1}{D_1}\left[s_1' - \rho_1\left(v_1^2 - u_1^2\right)\right]$$

$$D_1 = \frac{4\gamma}{\gamma^2 - 1} w_\infty^2 (1 - w_\infty^2)^{\frac{1}{\gamma - 1}} \frac{u_1 v_1 \sin 2\sigma}{1 - w_1^2}$$

$$+ \rho_1 \left\{ v_1 m_1 - u_1 \left[n_1 + \frac{2 v_1}{1 - w_1^2} (v_1 n_1 - u_1 m_1) \right] \right\}$$

$$m_1 = \frac{dw_y}{d\sigma} \sin\theta - \frac{dw_x}{d\sigma} \cos\theta ,$$

$$n_1 = - \frac{dw_x}{d\sigma} \sin\theta - \frac{dw_y}{d\sigma} \cos\theta \qquad \text{B2}$$

($dw_x/d\sigma$ and $dw_y/d\sigma$ are found from (1.12)

$$E_0 = \frac{2 c_0^2}{(\gamma + 1) r_0} t_0' \; ; \; E_i = \frac{2 c_i^2}{(\gamma + 1) t_i} \left(t_i' - M_i \frac{du_i}{d\theta} \right)$$

$$M_i = - \frac{t_i u_i}{c_i^2} \; ; \; c_i^2 = \frac{\gamma - 1}{2} (1 - w_i^2) \; ; \; G_1 = r_1 \left[\frac{v_1}{c_1^2} (v_1 n_1 - u_1 m_1) - n_1 \right]. \qquad \text{B3}$$

In the system (2.4), F , E_0 , E_i , s_i', and t_i' are holomorphic functions of θ and of the quantities required, and are defined in the range of integration (the form of these functions depends on N), and

$$\frac{d \ln \phi_i}{d\psi_i} = \frac{d \ln \phi_1}{d\psi_1} \Bigg|_{\psi_1 = \psi_i} = \frac{d \ln \phi_1}{d\sigma} \frac{d\sigma}{d\theta} \frac{d\theta}{d\psi_1} \Bigg|_{\psi_1 = \psi_i} \qquad \text{B4}$$

where $d \ln \phi_1 / d\sigma$ is determined from (1.14), $d\psi_1 / d\theta$ is determined from (1.15), and $d\sigma / d\theta = F$ is determined from (2.4).

We have thus obtained a system consisting of $3N$ ordinary differential equations and $N-1$ finite relations. All the boundary conditions on the body and on the shock wave are automatically satisfied, as can be seen from the scheme by which the approximating system has been constructed.

The integration of the resulting system is carried out numerically beginning at the axis of symmetry $\theta = 0$, where $\sigma = \pi/2$, $v_0 = v_i = \psi_i = 0$, while the N

initial values of the functions ϵ_0 and u_i ($i = 2, 3, \ldots, M$) are unknown (we have N parameters at $\theta = 0$). The problem of supersonic flow past bodies with a detached shock wave is of mixed type. As is well known, the distrubances that arise in the supersonic region past the boundary characteristic are not propagated in such problems into the subsonic region. We can therefore obtain no additional conditions for the determination of the remaining initial values of the functions required on the upper boundary of the region of integration. This fact is specifically reflected in the approximating system. It is seen from its structure that in the vicinity of the sonic line $\left(w_s^2 = \frac{\gamma - 1}{\gamma + 1}\right)$ the N equations of the system will have floating singular points, and special conditions must be satisfied if a continuous transition through these points is to be possible.

Actually, at points where $w_0^2 = \frac{\gamma - 1}{\gamma + 1}$ and $w_i^2 = \frac{\gamma - 1}{\gamma + 1} + \frac{2u_i^2}{\gamma + 1}$ (we shall call the set of these points the "singular line"), we should have respectively

$$E_0 = 0 \text{ and } E_i = 0 \ (i = 2, 3, \ldots, N) . \tag{2.5}$$

Otherwise the derivatives

$$\frac{dv_0}{d\theta}, \frac{dv_2}{d\theta}, \frac{dv_3}{d\theta}, \ldots, \frac{dv_N}{d\theta} \qquad \text{B5}$$

become infinite on the singular line; i.e., the accelerations become infinite, and the motion cannot continue past this line -- the singular line itself will be the limiting line, and all solutions will lose their physical meaning.

To satisfy the N conditions (2.5), we have at our disposal N parameters at $\theta = 0$. Thus, the requirement that the motion be continuous on the singular line indeed supplies us the conditions necessary to make the problem definite.

In reference 15, we investigated the character of the behavior of integral curves in the vicinity of the singular points (the singularities were of the "saddle" type). We also showed there that the approximating system (2.4) has a unique solution, is holomorphic in the entire region of integration, and satisfies the conditions at $\theta = 0$ and on the singular line.

We present computational formulas for $N = 1, 2, 3$.

First approximation ($N = 1$). There are no intermediate lines between the body and the wave (Fig. 2a).

The approximation is of the form

$$f(r,\theta) = f_0 + (f_1 - f_0)\frac{r-1}{\epsilon(\theta)} \qquad \text{B6}$$

where $f_0(\theta)$ and $f_1(\theta)$ are the values of $f(r,\theta)$ on the cylinder and on the wave, respectively. The unknowns are the functions ϵ, σ, v_0, and the functions that remain to be determined on the body and on the wave are found from the boundary conditions (1.11) and (1.13 - 1.15). The approximating system is readily obtained from (2.4) (first three equations). In this system

$$s_1' = \frac{1}{\epsilon}\left[s_1\frac{d\epsilon}{d\theta} + 2H_0 - 2(1+\epsilon)H_1\right] + g_0 + g_1$$

$$t_0' = \frac{1}{\epsilon}(t_1 - t_0)\frac{d\epsilon}{d\theta} - G_1\frac{d\sigma}{d\theta} - \left(1 + \frac{2}{\epsilon}\right)h_1 \qquad \text{B7}$$

When $\theta = 0$ we have $v_0 = 0$ and $\sigma = \pi/2$, while $\epsilon(0) = \epsilon_0$ is the one unknown parameter, determined from the following condition: we should have $E_0 = 0$ at the point A_0, where $v_0^2 = \frac{\gamma - 1}{\gamma + 1}$.

Second approximation (N = 2). We introduce one intermediate line (Fig. 2b).

The approximations

$$f(r,\theta) = f_0 + (4f_2 - f_1 - 3f_0)\frac{r-1}{\epsilon(\theta)}$$

$$+ 2(f_1 - 2f_2 + f_0)\left[\frac{r-1}{\epsilon(\theta)}\right]^2 \qquad \text{B8}$$

where $f_0(\theta)$, $f_1(\theta)$ and $f_2(\theta)$ are the values of $f(r,\theta)$ on the cylinder, on the wave, and on the central line, respectively. The unknown functions are ϵ, σ, v_0, u_2, v_2, ψ_2, and ϕ_2.

In the system (2.4) we have

$$s_1' = \frac{1}{\epsilon}\left\{(3s_1 - 4s_2)\frac{d\epsilon}{d\theta} - 4\left[H_0 + (1+\epsilon)H_1 - (2+\epsilon)H_2\right]\right\} + g_1 - g_0$$

$$s_2' = \frac{1}{2\epsilon}\left[s_1\frac{d\epsilon}{d\theta} + 5H_0 - (1+\epsilon)H_1 - 2(2+\epsilon)H_2\right] + \frac{\varepsilon_0}{2} + s_2$$

$$t_0' = t_1' + \frac{1}{\epsilon}\left\{4\left[(1+\epsilon)h_1 - (2+\epsilon)h_2\right] - (t_0 + 3t_1 - 4t_2)\frac{d\epsilon}{d\theta}\right\}$$

$$t_1' = G_1\frac{d\sigma}{d\theta} - h_1$$

$$t_2' = -\frac{t_1'}{2} + \frac{1}{\epsilon}\left[2(t_1 - t_2)\frac{d\epsilon}{d\theta} + (2+\epsilon)h_2 - \frac{5}{2}(1+\epsilon)h_1\right] . \qquad \text{B9}$$

When $\theta = 0$ we have $v_0 = v_2 = \psi_2 = 0$, $\sigma = \pi/2$, and ϵ_0 and $u_2(0)$ are the two unknown parameters, which are determined from the following conditions: at the point A_0, where $v^2 = (\gamma - 1)/(\gamma + 1)$ we should have $E_0 = 0$, and at the point A_2, where $w_2^2 = (\gamma - 1 + 2u_2^2)/(\gamma + 1)$, we should have $E_2 = 0$.

Third approximation (N = 3). We introduce two intermediate lines (Fig. 2c).

The approximations are

$$f(r,\theta) = f_0 + \frac{1}{2}(2f_1 - 11f_0 - 9f_2 + 18f_3)\frac{r-1}{\epsilon(\theta)} + \frac{9}{2}(2f_0 - f_1 + 4f_2 - 5f_3)\left[\frac{r-1}{\epsilon(\theta)}\right]^2 + \frac{9}{2}(f_1 - f_0 - 3f_2 + 3f_3)\left[\frac{r-1}{\epsilon(\theta)}\right]^3 \qquad \text{B10}$$

where $f_i(\theta) = f(r_i, \theta)$, $i = 0, 1, 2, 3$.

The unknown functions are

$$\epsilon, \sigma, v_0, u_2, v_2, u_3, v_3, \psi_2, \psi_3, \phi_2, \phi_3 . \qquad \text{B11}$$

The functions appearing in the right halves of the system (2.4) are of the form

$$s_1' = \frac{1}{16}(24A_2 - 13A_1 - 3A_3),\ s_2' = \frac{1}{12}(A_3 - A_1 - 4A_2),\ s_3' = \frac{1}{48}(A_1 - 8A_2 - A_3);$$

$$t_0' = \frac{1}{16}(24B_2 - 13B_1 - 3B_3 - 16t_1'),\ t_1' = G_1\frac{d\sigma}{d\theta} - h_1,\ t_2' = \frac{1}{48}(8B_2 - 17B_1 + B_3 - 16t_1')$$

$$t_3' = \frac{1}{24}(7B_1 - 16B_2 + B_3 + 8t_1')\ ;$$

$$A_1 = \frac{1}{\epsilon}\left\{\left[3(s_2 + s_3) - 7s_1\right]\frac{d\epsilon}{d\theta} + 8\left[(1+\epsilon)H_1 - H_0\right]\right\} - g_0 - g_1 - 3(g_2 + g_3),$$

$$A_2 = \frac{1}{\epsilon}\left\{(4s_3 - 5s_2)\frac{d\epsilon}{d\theta} + 9\left[\left(1 + \frac{2\epsilon}{3}\right)H_2 - H_0\right]\right\} - g_0 - g_2 - 4g_3\ ,$$

$$A_3 = \frac{1}{\epsilon}\left\{\left[s_1 - 5(s_2 + s_3)\right]\frac{d\epsilon}{d\theta} + 72\left[\left(1 + \frac{\epsilon}{3}\right)H_3 - H_0\right]\right\} - 9g_0 - g_1 + 5g_2 - 19g_3\ ;$$

$$B_1 = \frac{1}{\epsilon}\left\{\left[t_0 - 7t_1 + 3(t_2 + t_3)\right]\frac{d\epsilon}{d\theta} + 8(1+\epsilon)h_1\right\}\ ,$$

$$B_2 = \frac{1}{\epsilon}\left\{\left[t_0 - 5t_2 + 4t_3\right]\frac{d\epsilon}{d\theta} + 9\left(1 + \frac{2\epsilon}{3}\right)h_2\right\}\ ,$$

$$B_3 = \frac{1}{\epsilon}\left\{\left[9t_0 + t_1 - 5(t_2 + t_3)\right]\frac{d\epsilon}{d\theta} + 72\left(1 + \frac{\epsilon}{3}\right)h_3\right\}\ .$$

When $\theta = 0$ we have $v_0 = v_2 = v_3 = \psi_2 = \psi_3 = 0$, $\sigma = \pi/2$, and ϵ_0, $u_2(0)$, and $u_3(0)$ are the three unknown parameters, which are determined from the following three conditions:

$E_0 = 0$ at the point A_0, where $w_0^2 = (\gamma - 1)/(\gamma + 1)$

$E_2 = 0$ at the point A_2, where $w_2^2 = \left(\gamma - 1 + 2u_2^2\right)/(\gamma + 1)$

$E_3 = 0$, at the point A_3, where $w_3^2 = \left(\gamma - 1 + 2u_3^2\right)/(\gamma + 1)$.

To conclude this section, we note that in this problem it was found most convenient to use polar coordinates and to approximate the functions in terms of r. Also we have attempted to approximate the functions in terms of θ, and also introduced the coordinates ψ, ζ (ζ = const being orthogonal to ψ = const), ψ, x, and ξ, η ($\xi = (r - r_0(\theta))/\epsilon(\theta)$, $\eta = \theta/\theta_1(r)$, where $\theta_1(r)$ is the equation of the limiting characteristic), but the approximating systems obtained thereby were very unwieldy and had a large number of parameters. Next, if we take as the initial system of the differential equations a system equivalent to (2.4), in which the unknown functions are u, v, p, and ρ, we obtain an approximating system with $2N-1$ parameters at $\theta = 0$ and $2N-1$ conditions at the

singular points. During the formulation of the problem we carried out the calculation in a system like this, also, but even in the first approximation ($N \approx 1$) the results of the calculation were quite close to each other in both systems. For example, for $M_\infty = 5.0$ we had $\epsilon = 0.471$ in the system with the unknown functions u , v , ϕ and ψ , and $\epsilon = 0.481$ in the system with unknown u , v , p , and ρ .

III. TECHNIQUE OF COMPUTATION

The solution of the approximating system was carried out numerically with a varying number of intermediate lines. If the results of the last two approximations coincided with sufficient degree of accuracy, this was taken as evidence of the practical convergence of the computation. As already noted, integration of the system was carried out starting at the axis of symmetry $\theta = 0$, where $v_0 = v_i = \psi_i = 0$, $\sigma = \pi/2$ and ϵ_0 and $u_i(0)$ $(i = 2,3,\ldots,N)$ are the N unknown parameters. The principal difficulties in the calculations lie in the fact that, firstly, it is necessary to determine these N unknown parameters from the conditions on the singular line, and secondly that after one of these conditions is satisfied at each singular point, it is necessary to go numerically through this point (in the solution it is necessary to go through all the N singular points of the approximating system).

At each singular point, at least one of the equations of the system will have an indeterminate right-hand side (0/0) ; furthermore, the accuracy of the calculation of the right-hand sides becomes very poor in the vicinity of this point, and therefore ordinary methods of numerical integration become unsuitable. To make calculation possible there, the solution of the system in the vicinity of an arbitrary nonsingular (regular) point$(\theta(0), \epsilon(0), \sigma(0), \ldots, \phi_i(0))$ is expanded in powers of $\theta - \theta(0)$, and in the vicinity of a singular point$(\theta_k, \epsilon^*, \sigma^*, \ldots, \phi_i^*)$ it is expanded in powers of $\theta - \theta_k$ $(k = 0,2,3,\ldots,N)$. The convergence of such series was demonstrated elsewhere (15).

In the calculation, several steps ahead of the singular point on the integral curve (which is plotted in the ordinary manner) a regular point is selected $(\theta = \theta^{(0)}, \epsilon = \epsilon^{(0)}, \ldots, \phi_i = \phi_i^{(0)})$, and series are constructed in the vicinity of this regular point. These series are used to extend the solution to the singular point, then by variation of the parameter [at $k = 0$ the parameter is ϵ_0 , and at $k = 2,3,\ldots,N$ the parameter is $u_k(0)$] the required condition

$$E_k = 0 \text{ when } w_k^2 = (\gamma - 1 + 2u_k^2)/(\gamma + 1)$$

becomes satisfied at the k'th singular point. Thus we determine approximately the value of the parameter and the value of the quantities $\theta_k, \epsilon^*, \sigma^*, \ldots, \phi_i^*$, from which we then build up the series in the vicinity of the singular point. Using the condition that at $\theta = \theta^{(0)}$ these series must join the solution obtained in the oridnary manner, we refine by the method of iteration the values of the parameter and the values of the quantities $\theta_k, \epsilon^*, \sigma^*, \ldots, \phi_i^*$; the number of unknows in the iterations equals the number of conditions.

In the calculation of the flow around a circular cylinder, both types of series were constructed for $N = 1,2,3$. Examples of such series are given below for the first approximation. Furthermore, it is also known that if the singular

point is a "saddle," then, as the distance from the saddle increases, all the integral curves converge to two integral curves that pass through the singular point (in our problem only one such curve is joined to the solution ahead of the singular point). Using these series and the property of convergence of the integral curves, we succeeded in devising technically simple ways of passing through the singular points of the approximating system.

The system of ordinary differential equations was integrated numerically either by the Euler method with iteration or by the Runge-Kutta method. The integration was in steps of $\Delta\theta = 2^{-7}$ to 2^{-8}; the functions ϕ and $d \ln \phi/d\psi$ on the wave were fixed in steps of $\Delta\theta = 2^{-5}$ to 2^{-6}. The values of the functions $\phi_i(\psi_i)$ and $\frac{d \ln \phi_i}{d\psi_i}$ were found on the intermediate lines by quadratic interpolation from the values of the corresponding functions on the wave. The series for passing through the singular points were constructed in all approximations. For example, for $M_\infty = 5.0$ the series in the first approximation ($N = 1$) were of the following form:

In the vicinity of the regular point ($\theta^{(0)} = 0.81250$)

$$\epsilon = 0.72151 + 0.74562h + 0.73138h^2 + 0.70674h^3$$

$$\chi = 0.40377 + 0.44249h - 0.59405h^2 + 0.57399h^3$$

$$v_0 = 0.39980 + 0.40036h + 0.175163h^2 - 0.26982h^3 \qquad \text{C1}$$

and in the vicinity of the singular point ($\theta_0 = 0.85791$)

$$\epsilon = 0.75699 + 0.81704h + 0.74205h^2$$

$$\chi = 0.42264 + 0.40329h - 0.35727h^2$$

$$v_0 = 0.40825 + 0.37862h + 0.151850h^2 \qquad \text{C2}$$

where

$$\chi = \pi/2 - \sigma \quad \text{and} \quad h = \theta - \theta_0 .$$

The process of selecting two parameters from the conditions at the singular point was mechanized.

IV. RESULTS OF CALCULATIONS

The calculations for the flow past a circular cylinder were carried out for M_∞ = 2.13, 2.5, and 4.0 at N = 1 and 2, and for M_∞ = 3.0 and 5.0 at N = 1, 2, and 3. Some of the results of these calculations are presented here in graphs and in tables.

Figure 3 shows, for the case M_∞ = 3.0 and for the third approximation (N = 3), the shock wave, the sonic line (M = 1), and the limiting characteristics that bound the minimum region of influence. The region of influence will have a similar shape also for M_∞ = 2.5, 4.0, and 5.0. Figure 4 shows the dependence of ϵ_0 on M_∞ found in various approximations. Figures 5 and 6 show how the distribution of the pressure varies over the body, and also the shape and position of the shock wave and of the sonic line as M_∞ increases from 2.13 to 5.0 [here $p_0(\theta)/p_0(0)$ denotes the ratio of the pressure on the body to the pressure at the stagnation point] . The results are shown for the highest approximation for each value of M_∞ . For M_∞ = 2.13 and 2.5, no sonic lines were plotted since the calculations for these Mach numbers were carried out only for N = 1 and 2, and the accuracy of the determination of the sonic lines was found to be insufficient.

Figures 4, 7, 8, 9, and 10 illustrate the convergence of the method after various approximations for different values of M_∞ . Figure 4 shows the convergence of the method in finding the distance ϵ_0 , while figures 7 and 8 show the convergence in finding the pressure on the body and on the shock wave [$p_1(\theta)/p_1(0)$ denotes the ratio of the pressure on the wave to the pressure at its head] . Figures 9 and 10 give an idea of the accuracy of the calculation of the shape and position of the shock wave and sonic line in various approximations for M_∞ = 3.0 and M_∞ = 5.0.

Most papers, both here and abroad, have been devoted to a determination of the distance ϵ_0 from the surface of the body to the wave along the symmetry axis. Figure 11 shows a comparison of the results obtained experimentally and by calculations. It is seen that our results are in good agreement with the experimental data (for example, for M_∞ = 4.0 Kim (17) gives a value ϵ_0 = 0.54, while we get ϵ_0 = 0.546).

Figures 12, 13, and 14 give, for various values of M_∞ , a comparison with experiment of the pressure distribution over the body. The experiments for M_∞ = 2.5 and 3.0 were carried out by the scientific assistant G.M. Ryabinkov, while the experiments for M_∞ = 4.0 were carried out by Kim (17).

Figure 15 shows, for M_∞ = 4.0, the shock waves obtained by the method of integral relations (N = 2), using the theory of K. Tamada (8) and the experimentally obtained points (17). From all these comparisons, we see that the distribution of pressure over the body and the shape and position of the shock wave are in good agreement with experiment.

We now compare the sonic lines. Firstly, Kim (17) in his experimental work indicated that the sonic line is convex at $M_\infty = 4.0$. He wrote: "The sonic line is bent inside near the wave. It is not clear whether this is a very important property of the phenomenon, or whether it is caused by the fact that the shock wave is somewhat smeared out, a fact resulting from the action of the boundary layers on the window of the tube." Thus, the result we obtained (Fig. 6) is in qualitative agreement with Kim's result. Furthermore, in (15) we obtained correct expressions for the angles Φ_B between the lines $w = \text{const}$ and the direction of the incident stream in the plane case. It was shown there that on the shock wave these angles depend only on the magnitude of the velocity w and on the Mach number M_∞ of the incident stream. The magnitudes of these angles for different values $w = \text{const}$ (or $M = \text{const}$) and M_∞ are shown in figure 17. For the sonic line ($M = 1$), we have by calculation the following values for these angles: when $M_\infty = 3.0$, we have $\Phi_B \cong 20°$ ($N = 2$) and $\Phi_B = 1\text{-}2°$ ($N = 3$); when $M_\infty = 4$, $\Phi_B \cong 21\text{-}22°$ ($N = 2$), and when $M_\infty = 5.0$ we get $\Phi_B \cong 27\text{-}28°$ ($N = 2$). The exact values of the angle Φ_B for the same values of M_∞ are 3.312°, 19.840°, and 26.306°, respectively. Thus, for small values of M_∞ the accuracy with $N = 2$ is inadequate for plotting sonic lines, and when $M_\infty = 4.0$ and 5.0 even the second approximation gives sufficiently accurate results.

A Busemann suggested in his paper (6) that the sonic point on the body coincides with the point where the slope of the surface equals the critical angle of wedge or cone (for axially symmetrical flow), at which the frontal shock wave becomes detached. The positions of the sonic points, determined from this assumption, are compared in figure 16 with our own results. The same figure shows the experimental points, obtained by D. Holder and A. Chinneck (18), for $M_\infty = 1.42$, 1.60, and 1.79. It is seen from the graph that the sonic points, found by the method of A. Busemann, are located at much higher points on the body than the points obtained either by the method of integral relations or experimentally. Furthermore, it follows from the graph that as the Mach number M_∞ increases the sonic point shifts on the body towards the stagnation point, a fact to which Holder and Chinneck called attention.

An analysis of the calculation and a comparison of the results obtained with experiment show that in the vicinity of the axis of symmetry even the first approximation gives fair results. The distribution of pressure on the body and on the wave and the shape and position of the shock wave are all determined with sufficient accuracy over the entire region of integration by means of the second approximation; to construct the sonic lines at $M_\infty < 3.0$ to 3.5 we must have at least three approximations, while for $M_\infty > 3.5$ two approximations are sufficient.

The computed data make it possible to determine the distribution of the pressure on the surface and outside the body, the sonic line, the characteristics, the position and shape of the shock wave, and so on.

In conclusion, we tabulate the results of the calculations.

In Table I, we give the values of the following quantities as functions of the angle θ:

r -- distance from the body to the shock wave along θ = const

$\chi = \pi/2 - \sigma$ -- inclination of the wave to the vertical

$F_1(\psi) = \phi^{1/\gamma-1}$ -- entropy function (the entropy is $S = (\gamma - 1)\, c_v \ln F_1$)

$\frac{d \ln F_1(\psi)}{d\psi}$ -- derivative of the entropy function with respect to ψ

$p_0(\theta) / p_0(0)$ -- ratio of the pressure on the body to the pressure at the stagnation point.

Tables II, III, and IV list, for various M_∞, the values of the flow variables behind the shock wave at five points on the ray θ = const (the distance from the body to the wave along θ = const is divided into four parts:)

$\xi = \frac{r - 1}{\xi(\theta)}$ = 0 (body); 0.25; 0.50, 0.75, and 1.00 (shock wave)

$u, v,$ -- velocity components along r and θ

T, ρ, p -- temperature, density, and pressure

ψ -- stream function

$\Delta\theta$ $\approx 3.5°$.

Tables V and VI give the coordinates of the sonic line and of the limiting characteristic for various values of M_∞.

Table VII gives, for various values of M_∞, the values of the angles θ_{son} and θ_{char} at which the sonic line and the limiting characteristic intersect the surface of the body.

In all the tables, the angles are in radians, and the remaining quantities are in dimensionless form: linear dimensions are referred to the radius of the cylinder; the velocity is referred to the maximum velocity; the density, pressure, and temperature are referred to the corresponding stagnation values ahead of the shock wave.

REFERENCES

1. Smurov, G.S., Cylinder in supersonic stationary plane-parallel stream of gas. Trudy Voenno-vozdushnoi inzh. akademii im. N.E. Zhukovskovo (Trans. of Air Force Academy in name of N.E. Zhukovski) No. 191, 1947.

2. Panichkin, I.A., On the detached shock wave, Collection: Nekotorye zadachi gidro gazodinamiki (Certain problems of Hydro-gas dynamics) No. 67, Oborongiz, 1955.

3. Melkus, H., Über den abgelösten Verdichtungsstoss, Ingenieur-Archiv 19, No. 3, 1951.

4. Lin, C.C. and S.I. Rubinov, On the flow behind curved shocks, J. Math. Phys. 27, No. 2, 1948.

5. Guderley, G., Wright Field, Technical Report No. 39, 1947.

6. Busemann, A., A review of analytical methods for the treatment of flows with detached shocks, NACA TN 1858, 1949.

7. Hida, K., Asymptotic behaviour of the location of a detached shock wave in a nearly sonic flow, J. Phys. Soc. Jap. 10, No. 10, 1955.

8. Tamada, K., On detached shock wave of circular cylinder and sphere moving with supersonic velocities, Tomotika Lab., Techn. Mem. Faculty of Physics, No. 25, Univ. of Kyoto, 1950.

9. Hida, K., An approximate study on the detached shock wave in front of a circular cylinder and a sphere, J. Phys. Soc. Jap. No. 8, 1953; No. 1, 1955.

10. Kawamura, T., A note on the detached shock wave in front of a body, J. Jap. Soc. Appl. Mech. 5, Nos. 30-31, 1952-1953.

11. Uchida, S. and M. Yasuhara, The rotational field behind a curved shock wave calculated by the method of flux analysis, J. Aeronaut. Sci. 23, No. 9, 1956.

12. Maccoll, J.W. and J. Codd, Theoretical investigations of the flow around various bodies in the sonic region of velocities, British Armament Research Establishment, Theor. Res. Report, No. 17/45, 1945.

13. Mitchell, A.R., Application of relaxation to the rotational field of flow behind a bow shock wave, Quart. J. Mech. Appl. Math. 4, No. 3, 1951.

REFERENCES (Cont'd)

14. Dorodnitsyn, A. A., On a method of numerical solution of certain problems in aero-hydrodynamics, Trudy III Vsesoyuznovo mathmaticheskovo s'ezda (Trans. III All-Union Math. Congress), 2, 1956.

15. Belotserkovskii, O. M., Flow around a symmetrical profile with detached shock wave, Prikladnaya mathematika i mekhanika 22, No. 2, 1958; (Trans. in Applied Math. and Mech. No. 2, 1958).

16. Sauer, R., Introduction to Gas Dynamics, Edwards, Ann Arbor, 1947.

17. Kim, C.S., Experimental studies of supersonic flow past a circular cylinder, J. Phys. Soc. Jap. 11, No. 4,1956.

18. Holder, D. and A. Chinnek, The flow past elliptic-nosed cylinders and bodies of revolution in supersonic air streams, Aero. Quart. 4 (4), 317-340 (1954).

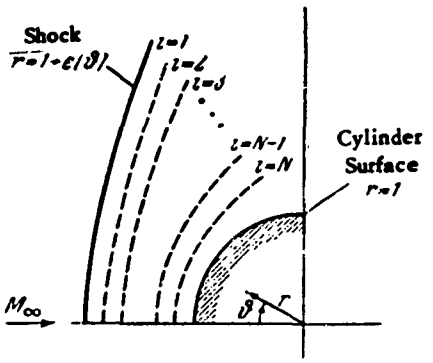

Figure 1

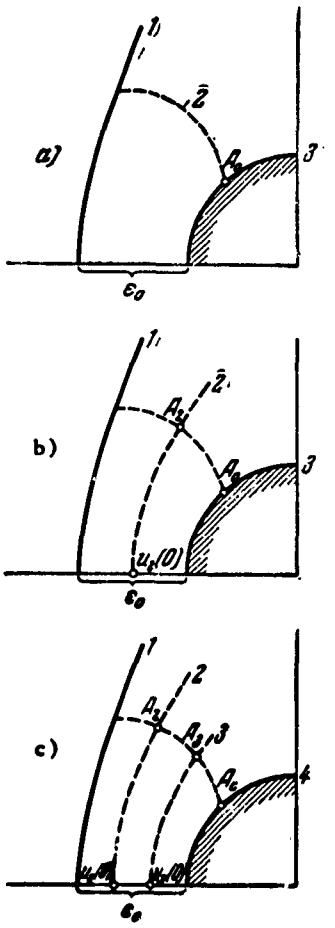

Figure 2

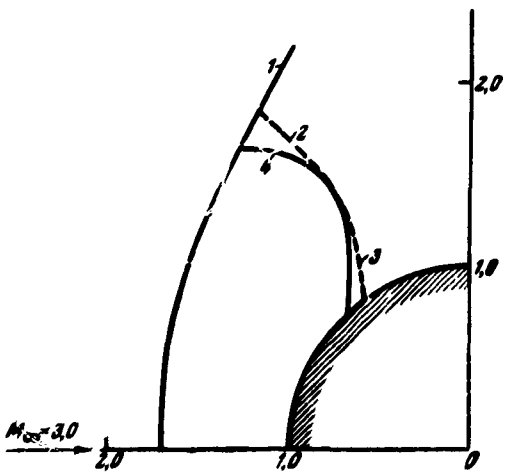

Figure 3

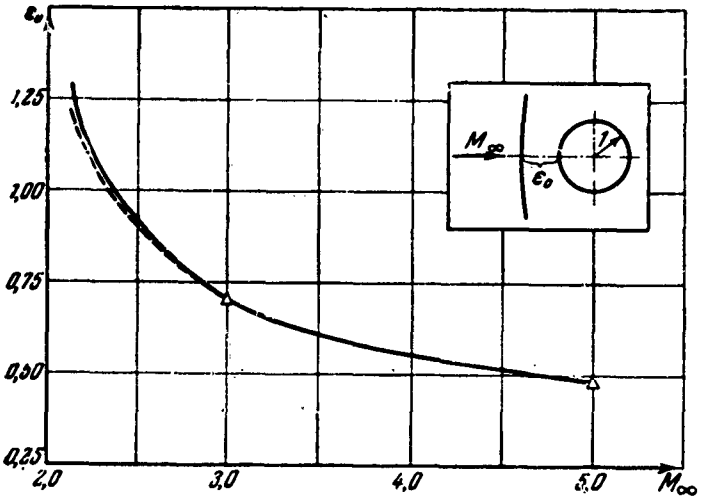

Figure 4

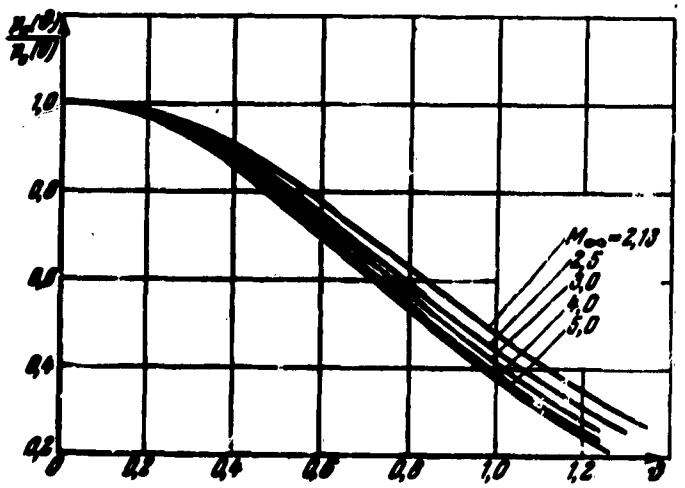

Figure 5

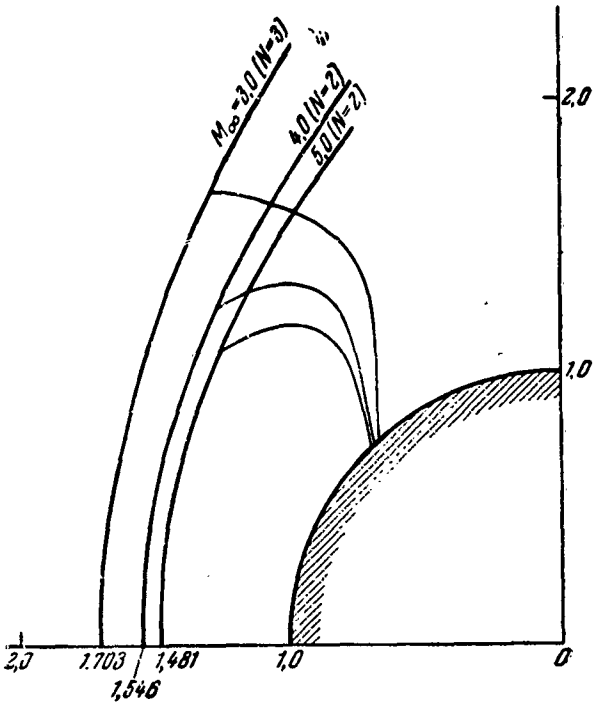

Figure 6

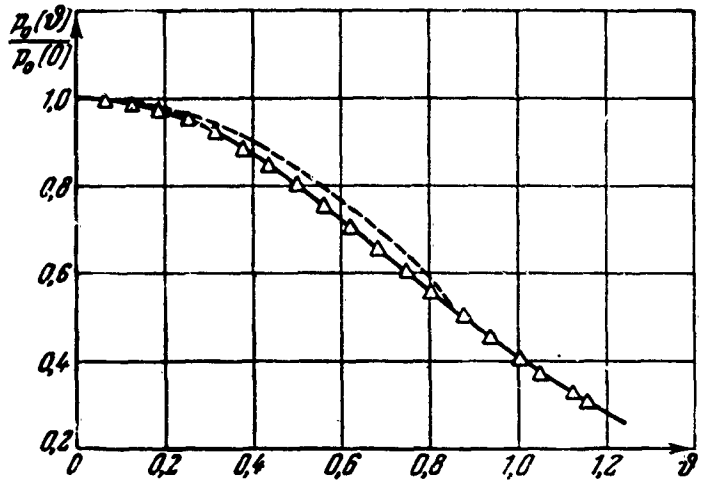

Figure 7

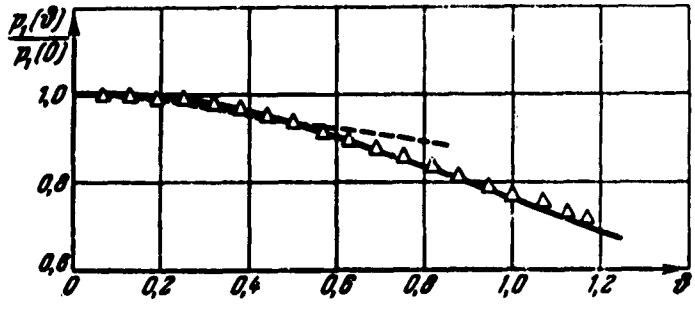

Figure 8

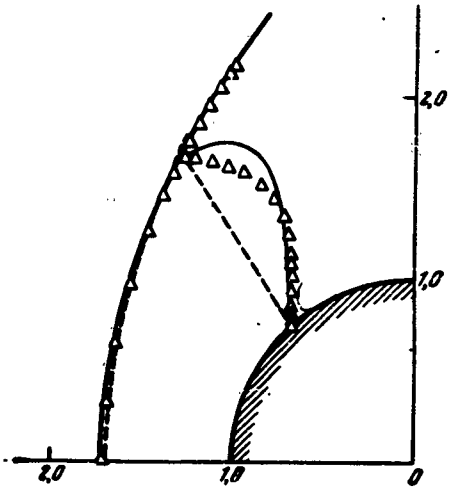

Figure 9

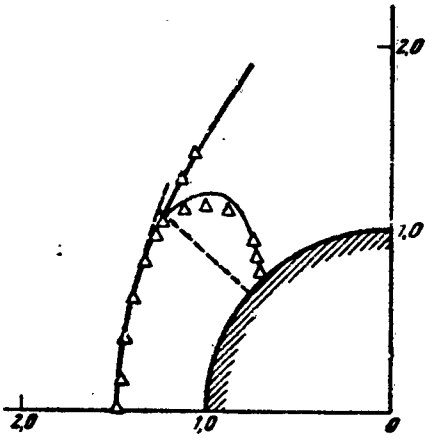

Figure 10

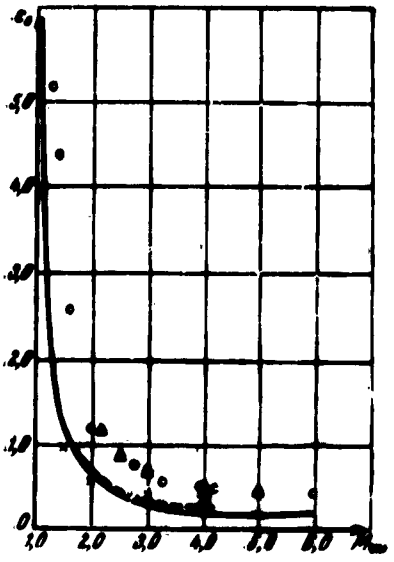

Figure 11

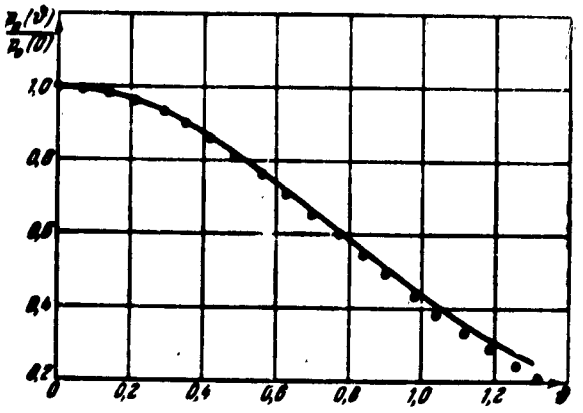

Figure 12

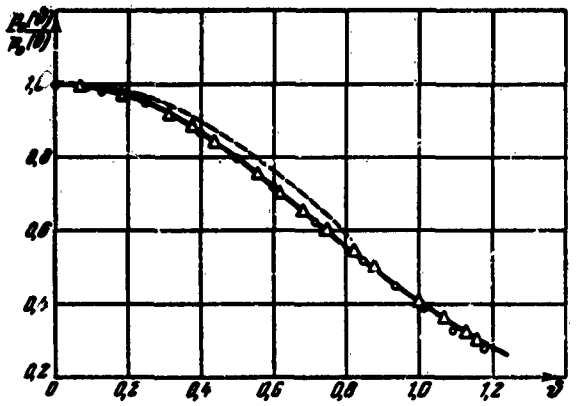

Figure 13

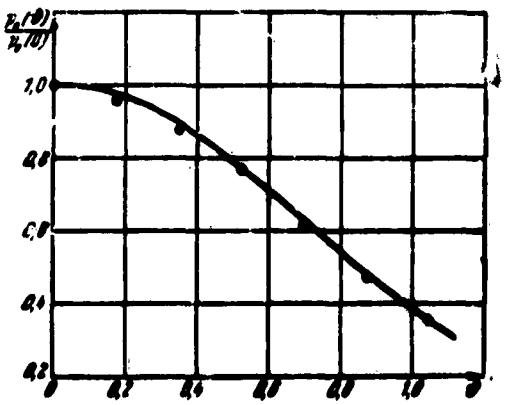

Figure 14

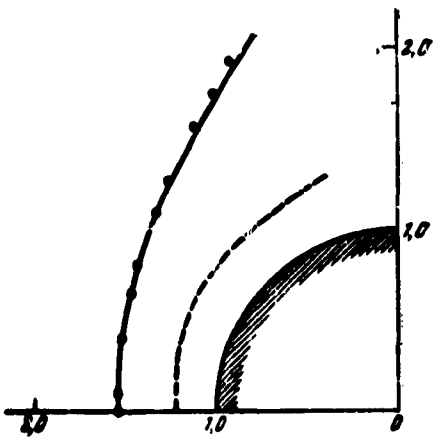

Figure 15

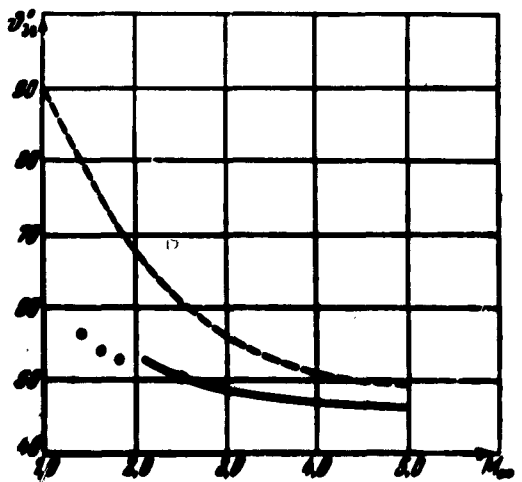

Figure 16

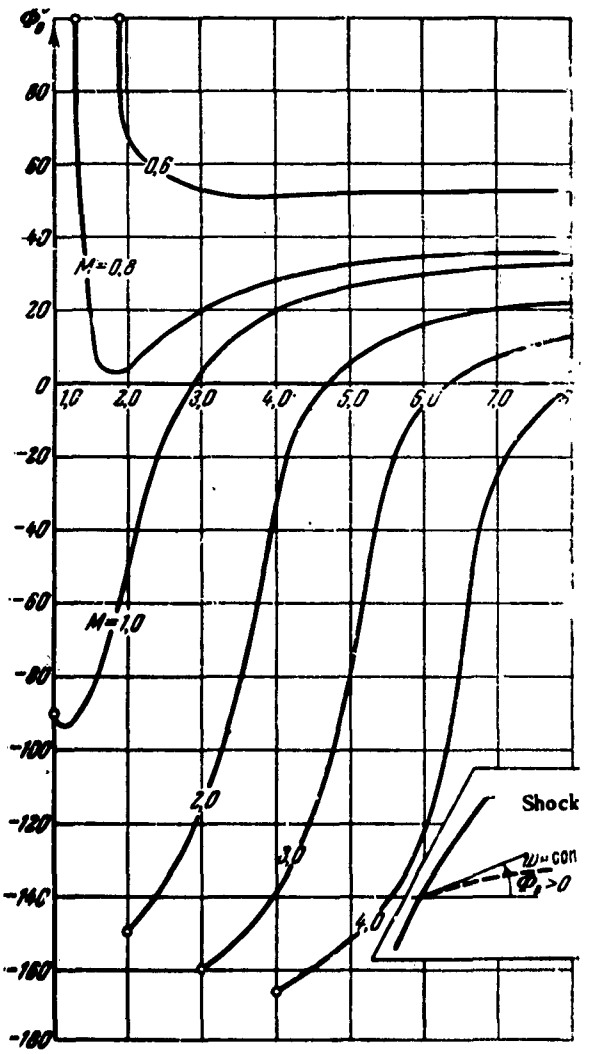

Figure 17

TABLE I

Φ	ε	x	F_2	$\frac{d \ln F_2}{d\Phi}$	$p_c(\Phi)/p_c(0)$
			$M_\infty = 2,5$		
0,0000	0,913	0,0000	2,004	—0,0000	1,000
625	915	0231	003	— 0926	0,997
1250	922	0476	1,999	— 208	990
1875	933	0749	992	— 362	978
2500	949	105	981	— 549	959
0,3125	0,969	0,137	1,966	—0,744	0,933
3750	993	170	946	— 919	900
4375	1,021	204	922	—1,056	863
5000	053	236	896	— 157	820
5625	090	267	867	— 228	775
0,6250	1,132	0,297	1,836	—1,278	0,728
6875	181	326	805	— 314	679
7500	235	355	772	— 338	629
8125	297	382	739	— 348	580
8633	354	404	711	— 346	541
0,8945	1,391	0,418	1,694	—1,398	0,518
9375	446	436	670	— 325	485
1,0000	535	462	636	— 287	439
0625	636	487	602	— 246	396
1250	749	512	568	— 188	356
1,1875	1,878	0,536	1,535	—1,118	0,318
2500	2,025	559	503	— 039	284
2812	106	570	487	—0,997	267
			$M_\infty = 3,0$		
0,0000	0,703	0,0000	3,046	—0,000	1,000
0625	704	0330	041	— 486	0,996
1250	709	0694	027	— 926	987
1875	716	102	004	—1,323	970
2500	727	135	2,975	— 714	947
0,3125	0,741	0,167	2,937	—2,102	0,918
3750	759	200	893	— 461	883
4375	780	232	843	— 774	844
5000	805	263	787	—3,038	801
5625	834	294	727	— 256	754
0,6250	0,866	0,324	2,664	—3,432	0,706
6675	907	354	598	— 565	655
7207	930	369	562	— 619	628
7520	952	384	528	— 658	603
7832	977	398	493	— 685	578

TABLE I (Cont'd)

ψ	ϵ	τ	F_1	$-\frac{d \ln F_1}{d\psi}$	$\rho_0(\theta)/\rho_0(0)$
0,8145	1,003	0,412	2,459	—3,609	0,552
8379	023	422	433	— 699	533
8750	057	439	391	— 724	504
9062	088	452	356	— 719	479
9375	121	466	321	— 706	455
0,9688	1,156	0,479	2,286	—3,682	0,431
1,0000	193	493	251	— 650	408
0312	232	506	217	— 587	385
0625	274	518	183	— 501	363
0938	318	531	149	— 408	342
1,1250	1,365	0,543	2,117	—3,322	0,321
1562	415	555	084	— 230	301
			$M_\infty = 4,0$		
0,0000	0,546	0,0000	7,207	— 0,000	1,000
0625	548	0323	194	— 1,541	0,996
1250	552	0665	153	— 3,414	987
1875	559	103	078	— 5,618	970
2500	569	141	6,967	— 7,825	945
0,3125	0,580	0,180	6,823	— 9,762	0,913
3750	595	217	654	—11,385	876
4375	612	253	464	—12,785	834
5000	632	289	259	—14,035	788
5625	656	323	041	—15,172	739
0,6250	0,683	0,357	5,813	—16,198	0,688
6875	714	390	577	—17,096	636
7500	749	422	336	— 855	584
8008	780	448	139	—18,305	542
8438	810	470	4,971	— 998	507
0,8750	0,832	0,485	4,849	—18,885	0,482
9375	882	516	609	—19,085	433
1,0000	936	546	373	—19,102	386
0625	1,001	575	144	—18,970	343
1250	071	603	3,923	— 705	303
1,1875	1,150	0,631	3,709	—18,308	0,266
			$M_\infty = 5,0$		
0,0000	0,431	0,0000	16,203	— 0,0000	1,000
0625	483	0343	166	— 4,8485	0,996
1250	486	0707	047	—10,745	986
1875	493	109	15,831	—17,490	968
2500	501	149	517	—24,000	942

TABLE I (Cont'd)

ψ	ξ	z	F_1	$\frac{d \ln F_1}{d\psi}$	$p_0(\psi)/p_0(0)$
0,3125	0,512	0,189	15,118	—29,650	0,909
3750	524	227	14,655	—34,520	871
4375	540	265	139	—38,900	827
5000	558	301	13.584	—42,940	780
5625	579	337	12,997	—46,680	730
0,6250	0,603	0,371	12,386	—50,120	0,679
6875	631	406	11,759	—53,220	625
7500	662	439	125	—55,920	572
8125	698	472	10,488	—58,220	522
8750	738	505	9,856	—60,100	468
0,9375	0,782	0,536	9,237	—61,520	0,418
1,0000	832	567	8,634	—62,380	372
0625	888	598	053	— 650	328
1250	951	627	7,496	— 250	288
1875	1,021	656	6,969	—61,080	251

TABLE II

ψ	u	v	T	ρ	p	Φ
			$\xi = 0,00$			
0,0000	0,0000	0,0000	1,0000	0,328	0,328	0,0000
0625	0000	0299	0,999	327	327	0000
1250	0000	0607	998	325	324	0000
1875	0000	0921	991	321	318	0000
2500	0000	123	984	315	311	0000
0,3125	0,0000	0,155	0,975	0,308	0,301	0,0000
3750	0000	186	965	300	290	0000
4375	0000	217	952	.290	277	0000
5000	0000	247	936	280	263	0000
5625	0000	277	922	268	247	0000
0,6250	0,0000	0,307	0,905	0,256	0,231	0,0000
6875	0000	336	886	242	215	0000
7207	0000	352	875	235	206	0000
7520	0000	366	865	228	198	0000
7832	0000	380	855	221	189	0000

TABLE II (Cont'd)

θ	u	v	T	ρ	p	ψ
0,8145	0,0000	0,394	0,841	0,214	0,181	0,0000
8379	0000	405	835	209	175	0000
8750	0000	421	822	201	165	0000
9062	0000	435	810	194	157	0000
9375	0000	448	798	187	149	0000
0,9688	0,0000	0,462	0,786	0,180	0,141	0,0000
1,0000	0000	475	774	173	134	0000
0312	0000	488	761	166	126	0000
0625	0000	501	749	159	119	0000
0938	0000	513	736	152	112	0000
1,1250	0,0000	0,526	0,722	0,145	0,105	0,0000
1562	0000	538	709	139	0988	0000
			$\xi = 0,25$			
0,0000	—0,0706	0,0000	0,995	0,323	0,322	0,0000
0625	— 0703	0286	994	323	321	00168
1250	— 0697	0570	991	321	319	00337
1875	— 0685	0850	988	318	314	00505
2500	— 0667	112	982	314	309	00673
0,3125	—0,0643	0,140	0,976	0,309	0,302	0,00839
3750	— 0612	167	968	303	294	0100
4375	— 0574	193	959	297	285	0116
5000	— 0529	219	948	289	274	0132
5625	— 0477	245	937	281	264	0148
0,6250	—0,0417	0,270	0,925	0,273	0,252	0,0164
6875	— 0348	294	912	263	240	0179
7207	— 0308	306	905	258	234	0187
7520	— 0268	317	898	254	228	0194
7832	— 0226	329	891	249	222	0201
0,8145	—0,0181	0,339	0,884	0,244	0,216	0,0209
8379	— 0146	348	878	241	211	0214
8750	— 00876	360	870	235	204	0223
9062	— 00353	370	862	230	198	0230
9375	00194	380	855	225	193	0237
0,9688	0,00769	0,390	0,847	0,221	0,187	0,0244
1,0000	0137	399	840	216	181	0251
0312	0199	408	832	211	176	0257
0625	0265	417	824	206	170	0264
0938	0334	426	817	202	165	0271
1,1250	0,0405	0,434	0,809	0,197	0,159	0,0278
1562	0479	442	801	192	154	0285

TABLE II (Cont'd)

η	u	v	T	ρ	p	ϕ
			$\xi = 0,50$			
0,0000	—0,122	0,0000	0,984	0,316	0,311	0,0000
0625	— 122	0282	984	316	311	00327
1250	— 121	0561	982	314	309	00654
1875	— 118	0839	978	312	306	00981
2500	— 115	111	974	309	301	0130
0,3125	—0,111	0,138	0,968	0,306	0,296	0,0163
3750	— 105	164	961	301	290	0195
4375	— 0996	191	953	297	283	0227
5000	— 0921	216	944	291	275	0260
5625	— 0835	241	934	285	267	0292
0,6250	—0,0738	0,264	0,924	0,279	0,258	0,0324
6875	— 0629	288	913	273	249	0355
7207	— 0566	299	906	269	244	0372
7520	— 0503	310	900	266	239	0388
7832	— 0438	321	894	262	235	0404
0,8145	—0,0369	0,331	0,888	0,259	0,230	0,0420
8379	— 0316	339	883	256	226	0432
8750	— 0227	350	876	252	221	0451
9062	— 0149	360	869	249	216	0467
9375	— 00684	369	863	245	212	0484
0,9688	0,00161	0,378	0,856	0,242	0,207	0,0500
1,0000	0103	387	850	238	202	0516
0312	0194	395	843	235	196	0533
0625	0288	403	836	231	193	0550
0938	0385	411	829	228	189	0567
1,1250	0,0485	0,418	0,822	0,224	0,184	0,0584
1562	0588	425	815	221	180	0601
			$\xi = 0,75$			
0,0000	—0,166	0,0000	0,972	0,305	0,297	0,0000
0625	— 165	0295	971	305	297	00485
1250	— 162	0591	969	305	295	00970
1875	— 159	0887	966	303	293	0145
2500	— 154	118	962	301	290	0194
0,3125	—0,149	0,148	0,956	0,299	0,286	0,0242
3750	— 141	175	949	296	281	0291
4375	— 133	202	941	293	276	0340
5000	— 123	229	932	289	270	0389
5625	— 111	255	922	285	263	0439
0,6250	—0,0990	0,280	0,911	0,281	0,256	0,0489
6875	—0850	304	899	276	248	0539

TABLE II (Cont'd)

ϑ	u	v	T	ρ	p	ψ
7207	— 0771	317	893	273	244	0566
7520	— 0692	328	887	271	240	0592
7832	— 0611	339	881	268	236	0618
0,8145	—0,0526	0,350	0,874	0,266	0,232	0,0644
8379	— 0461	358	869	264	229	0664
8750	— 0354	370	861	261	225	0695
9062	— 0260	380	854	258	220	0722
9375	— 0164	389	848	255	216	0750
0,9688	—0,00644	0,398	0,841	0,252	0,212	0,077?
1,0000	00376	407	833	250	208	0806
0312	0142	415	826	247	204	0834
0625	0250	424	819	244	200	0863
0938	0360	431	812	241	196	0893
1,1250	0,0472	0,439	0,804	0,238	0,192	0,0924
1562	0585	446	797	235	188	0955

$\xi = 1{,}00$

0,0000	—0,207	0,0000	0,956	0,294	0,281	0,0000
0625	— 207	0337	956	293	280	00650
1250	— 204	0671	953	293	279	0130
1875	— 199	0995	950	292	278	0195
2500	— 193	131	945	292	276	0261
0,3125	—0,185	0,162	0,939	0,291	0,273	0,0327
3750	— 175	192	931	289	269	0393
4375	— 164	222	923	288	266	0461
5000	— 151	251	914	286	261	0529
5625	— 136	278	903	284	257	0598
0,6250	—0,120	0,305	0,892	0,282	0,252	0,0668
6875	— 102	329	880	280	246	0739
7207	— 0822	342	874	279	243	0778
7520	— 0623	353	868	277	241	0815
7832	— 0720	364	861	276	238	0852
0,8145	—0,0615	0,375	0,855	0,275	0,235	0,0890
8379	— 0539	383	850	274	233	0919
8750	— 0400	394	842	272	229	0965
9062	— 0285	404	835	271	226	100
9375	— 0167	413	829	269	223	104
0,9688	—0,00468	0,421	0,822	0,268	0,220	0,108
1,0000	00765	429	815	266	217	112
0312	0203	437	808	264	214	117
0625	0331	444	801	263	210	121
0938	0463	451	794	261	207	125
1,1250	0,0596	0,457	0,787	0,260	0,204	0,130
1562	0732	462	780	258	201	135

TABLE III

η	u	v	T	ρ	p	ϕ
			$\xi = 0{,}00$			
0,0000	0,0000	0,0000	1,000	0,138	0,138	0,0000
0625	0000	0292	0,999	138	138	0000
1250	0000	0598	996	137	137	0000
1875	0000	0923	991	135	134	0000
2500	0000	125	984	133	131	0000
0,3125	0,0000	0,159	0,974	0,130	0,126	0,0000
3750	0000	192	963	126	121	0000
4375	0000	224	949	121	115	0000
5000	0000	256	934	117	109	0000
5625	0000	287	917	111	102	0000
0,6250	0,0000	0,317	0,899	0,106	0,0956	0,0000
6875	0000	347	879	100.	0883	0000
7500	0000	377	857	0946	0811	0000
8008	0000	400	839	0895	0752	0000
8438	0000	419	824	0855	0704	0000
0,8750	0,0000	0,433	0,811	0,0823	0,0668	0,0000
9375	0000	461	787	0763	0601	0000
1,0000	0000	487	762	0704	0536	0000
0625	0000	512	736	0646	0476	0000
1250	0000	537	711	0592	0421	0000
1,1875	0,0000	0,561	0,685	0,0539	0,0369	0,0000
			$\xi = 0{,}25$			
0,0000	—0,0564	0,0000	0,996	0,137	0,136	0,0000
0625	— 0563	0307	995	136	136	000571
1250	— 0559	0611	993	135	135	00114
1875	— 0549	0912	988	134	133	00171
2500	— 0534	120	982	132	130	00228
0,3125	—0,0513	0,150	0,974	0,130	0,126	0,00284
3750	— 0487	179	965	127	122	00338
4375	— 0455	207	954	123	118	00392
5000	— 0417	235	942	120	113	00445
5625	— 0372	263	929	116	107	00496
0,6250	—0,0319	0,289	0,915	0,111	0,102	0,00545
6875	— 0260	315	899	107	0966	00593
7500	— 0192	340	883	102	0908	00638
8008	— 0131	360	869	0969	0860	00674
8438	— 00754	376	858	0957	0821	00703
0,8750	—0,00321	0,388	0,849	0,0932	0,0792	0,00723
9375	00606	410	831	0885	0736	00762
1,0000	0162	431	813	0837	0681	00799
0625	0272	450	795	0790	0628	00834
1250	0391	469	778	0744	0579	00866
1,1875	0,0520	0,487	0,760	0,0699	0,0531	0,00896

TABLE III (Cont'd)

θ	u	v	T	ρ	p	ψ
			$\xi = 0,50$			
0,0000	—0,106	0,0000	0,985	0,134	0,133	0,000
0625	— 106	0319	987	134	132	00115
1250	— 105	0631	984	133	131	00230
1875	— 103	0931	980	132	130	00345
2500	— 100	122	975	131	127	00460
0,3125	—0,0963	0,150	0,968	0,129	0,125	0,00574
3750	— 0911	178	959	127	122	00687
4375	— 0848	206	950	125	118	00798
5000	— 0773	233	939	122	115	00908
5625	— 0687	259	928	119	111	0101
0,6250	—0,0588	0,284	0,915	0,117	0,107	0,0112
6875	— 0477	309	902	113	102	0122
7500	— 0352	332	888	110	0985	0133
8008	— 0241	350	876	108	0949	0141
8438	— 0140	364	866	106	0919	0148
0,8750	—0,00626	0,374	0,859	0,104	0,0897	0,0153
9375	0,0102	394	844	101	0854	0162
1,0000	0281	412	829	0978	0811	0172
0625	0474	428	814	0945	0769	0181
1250	0680	443	798	0913	0729	0190
1,1875	0,0900	0,457	0,782	0,0879	0,0688	0,0199
			$\xi = 0,75$			
0,0000	—0,151	0,0000	0,977	0,131	0,128	0,0000
0625	— 151	0330	976	131	127	00173
1250	— 149	0657	973	130	127	00348
1875	— 146	0979	969	129	125	00522
2500	— 141	129	963	129	124	00696
0,3125	—0,134	0,160	0,956	0,128	0,122	0,00870
3750	— 127	190	947	126	120	0104
4375	— 117	220	937	125	117	0121
5000	— 107	248	926	124	115	0139
5625	— 0946	276	914	122	112	0156
0,6250	—0,0807	0,302	0,902	0,120	0,109	0,0173
6875	— 0651	327	888	119	105	0190
7500	— 0481	351	874	117	102	0207
8008	— 0330	369	862	116	100	0221
8438	— 0194	383	852	114	0977	0233
0,8750	—0,00915	0,393	0,844	0,113	0,0961	0,0242
9375	0,0125	412	829	111	0928	0259
1,0000	0358	430	813	109	0895	0276
0625	0616	445	797	107	0861	0294
1250	0867	459	781	105	0828	0312
1,1875	0,114	0,471	0,764	0,103	0,0794	0,0330

TABLE III (Cont'd)

θ	u	v	T	ρ	p	ϕ
			$\xi = 1{,}00$			
0,0000	—0,190	0,0000	0,963	0,126	0,121	0,0000
0625	— 189	0339	962	126	121	00233
1250	— 187	0690	960	126	121	00467
1875	— 182	105	955	126	120	00701
2500	— 175	143	948	125	119	00937
0,3125	—0,167	0,179	0,939	0,125	0,117	0,0117
3750	— 156	215	928	124	116	0141
4375	— 144	249	916	124	114	0164
5000	— 130	282	903	123	111	0189
5625	— 114	313	888	123	109	0213
0,6250	—0,0976	0,343	0,872	0,122	0,106	0,0237
6875	— 0783	371	855	121	104	0262
7500	— 0577	397	838	120	101	0287
8008	— 0397	417	823	119	0987	[illegible]
8438	— 0238	434	810	119	0966	0326
0,8750	—0,0118	0,445	0,801	0,118	0,0950	0,0339
9375	0129	466	782	117	0918	0366
1,0000	0392	485	762	116	0886	0393
0625	0666	502	743	114	0854	0422
1250	0950	517	723	113	0821	0451
1,1875	0,124	0,529	0,704	0,112	0,0789	0,0481

TABLE IV

θ	u	v	T	ρ	p	ϕ
			$\xi = 0{,}00$			
0,0000	0,0000	0,0000	1,000	0,0617	0,0617	0,0000
0625	0000	0000	0,999	0615	0615	0000
1250	0000	0017	996	0611	0609	0000
1875	0000	0062	990	0603	0597	0000
2500	0000	129	983	0591	0581	0000
0,3125	0,0000	0,198	0,973	0,0576	0,0561	0,0000
3750	0000	196	961	0559	0537	0000
4375	0000	229	947	0539	0510	0000
5000	0000	261	931	0517	0481	0000
5625	0000	292	914	0493	0451	0000
0,6250	0,0000	0,323	0,895	0,0468	0,0419	0,0000
6875	0000	354	874	0441	0386	0000
7500	0000	383	852	0414	0353	0000
8125	0000	411	830	0386	0322	0000
8750	0000	441	805	0359	0289	0000

TABLE IV (Cont'd)

ϕ	u	v	T	ρ	p	ϕ
0,9375	0,0000	0,469	0,779	0,0331	0,0258	0,0000
1,0000	0000	496	754	0304	0229	0000
0625	0000	522	727	0278	0202	0000
1250	0000	547	700	0253	0177	0000
1875	0000	570	674	0230	0155	0000
			$\xi = 0,25$			
0,0000	—0,0519	0,0000	0,997	0,0611	0,0609	0,0000
0625	— 0520	0316	996	0610	0607	000230
1250	— 0514	0630	993	0605	0601	000460
1875	— 0504	0939	988	0598	0592	000688
2500	— 0489	124	982	0589	0578	000915
0,3125	—0,0469	0,154	0,973	0,0577	0,0562	0,00113
3750	— 0444	184	964	0563	0543	00135
4375	— 0413	213	952	0547	0521	00156
5000	— 0376	242	939	0530	0498	00177
5625	— 0333	270	925	0511	0473	00197
0,6250	—0,0282	0,298	0,910	0,0491	0,0447	0,00216
6875	— 0224	325	893	0470	0420	00235
7500	— 0158	350	876	0448	0393	00252
8125	— 00842	374	859	0426	0366	00269
8750	— 000141	399	840	0403	0339	00284
0,9375	0,00808	0,421	0,822	0,0381	0,0313	0,00298
1,0000	0190	443	803	0358	0288	00311
0625	0269	463	784	0336	0264	00323
1250	0417	482	765	0315	0241	00334
1875	0545	500	747	0294	0220	00344
			$\xi = 0,50$			
0,0000	—0,0697	0,0000	0,990	0,0602	0,0596	0,0000
0625	— 0696	0632	989	0600	0594	000466
1250	— 0693	0955	986	0597	0588	000933
1875	— 0682	0966	981	0591	0580	00139
2500	— 0660	128	975	0584	0570	00186
0,3125	—0,0630	0,156	0,967	0,0576	0,0558	0,00232
3750	— 0595	186	958	0567	0543	00277
4375	— 0775	214	947	0555	0526	00321
5000	— 0702	243	936	0543	0509	00365
5625	— 0617	270	923	0530	0489	00408
0,6250	—0,0519	0,296	0,909	0,0516	0,0469	0,00450
6875	— 0408	322	894	0502	0449	00492
7500	— 0285	346	879	0487	0428	00532
8125	— 0147	368	863	0472	0407	00571
8750	0,000	390	847	0456	0386	00609

TABLE IV (Cont'd)

ϑ	u	v	T	p	ρ	φ
0,9375	0,0168	0,410	0,831	0,0441	0,0366	0,00646
1,0000	0347	428	815	0425	0346	00682
0625	0540	445	798	0409	0327	00716
1250	0747	461	781	0394	0308	00750
1875	0968	474	765	0378	0289	00782
			$\xi = 0,75$			
0,0000	—0,143	0,0000	0,979	0,0587	0,0575	0,0000
0625	— 142	0348	978	0586	0573	000709
1250	— 140	0693	975	0584	0569	00141
1875	— 137	103	970	0581	0564	00212
2500	— 132	136	963	0577	0556	00283
0,3125	—0,125	0,169	0,955	0,0572	0,0547	0,00354
3750	— 118	201	945	0567	0536	00424
4375	— 108	232	934	0561	0524	00494
5000	— 0977	262	921	0555	0511	00564
5625	— 0852	291	907	0547	0497	00633
0,6250	—0,0711	0,319	0,893	0,0540	0,0482	0,00702
6875	— 0554	345	877	0532	0467	00771
7500	— 0381	370	861	0524	0451	00839
8125	— 0191	393	844	0515	0435	00907
8750	0,00144	414	828	0507	0420	00975
0,9375	0,0235	0,434	0,810	0,0498	0,0404	0,0104
1,0000	0472	452	793	0490	0388	0111
0625	0723	468	775	0481	0372	0117
1250	0990	482	757	0471	0357	0124
1875	127	495	738	0462	0341	0131
			$\xi = 1,00$			
0,0000	—0,182	0,0000	0,966	0,0567	0,0548	0,0000
0625	— 181	0364	965	0566	0547	000958
1250	— 178	0743	962	0566	0545	00191
1875	— 173	113	956	0565	0541	00286
2500	— 166	153	948	0564	0535	00384
0,3125	—0,158	0,192	0,937	0,0563	0,0528	0,00481
3750	— 147	230	925	0562	0520	00578
4375	— 134	266	910	0560	0510	00675
5000	— 120	300	895	0558	0499	00773
5625	— 103	333	877	0555	0487	00872
0,6250	—0,0858	0,364	0,859	0,0553	0,0475	0,00971
6875	— 0659	394	840	0550	0462	0107
7500	— 0445	422	819	0546	0448	0117
8125	— 0213	448	798	0543	0433	0127
8750	0,00317	472	776	0539	0419	0138

TABLE IV (Cont'd)

θ	u	v	T	ρ	p	ψ
0,9375	0,0291	0,494	0,754	0,0535	0,0404	0,0148
1,0000	0563	514	731	0531	0388	0159
0625	0849	532	709	0526	0373	0170
1250	114	548	686	0521	0357	0182
1875	145	561	664	0516	0342	0194

TABLE V

$M_\infty = 3,0$		$M_\infty = 4,0$		$M_\infty = 5,0$	
$-x$	y	$-x$	y	$-x$	$+y$
0,664	0,748	0,681	0,732	0,693	0,721
666	798	692	778	710	798
668	852	704	843	724	867
669	911	716	914	745	951
670	974	731	995	786	1,055
0,671	1,045	0,757	1,102	0,815*	1,097
677	135	800*	217	830	113
692	246	886	290	909	160
720	340	965	314	944	167
777*	443	1,029	314	976	169
0,841	1,510	1,086	1,302	1,006	1,167
940	569	143	284	034	162
1,029	602	163	276	067	148
117	626	181	266	136	128
270	668	266	222	247	068

TABLE VI

$M_\infty = 3,0$		$M_\infty = 4,0$		$M_\infty = 5,0$	
$-x$	y	$-x$	y	$-x$	y
0,575	0,818	0,628	0,778	0,649	0,761
576	834	643	837	656	784
584	904	661	901	667	816
593	972	682	964	678	847
605	1,038	704	1,024	690	877

TABLE VI (Cont'd)

$M_\infty = 3,0$		$M_\infty = 4,0$		$M_\infty = 5,0$	
$-x$	y	$-x$	y	$-x$	y
0,620	1,101	0,717	1,054	0,702	0,907
638	163	730	082	716	937
660	222	744	111	730	965
684	280	759	138	745	993
711	336	775	165	761	1,020
0,742	1,391	0,792	1,192	0,778	1,046
777	443	809	217	796	072
				815	097
		II			
0,777	1,443	0,809	1,217	0,815	1,097
813	494	828	242	835	121
853	544	848	267	856	144
896	592	869	290	879	166
941	638	891	313	903	187
0,988	1,683	0,915	1,335	0,928	1,206
1,037	726	939	356	955	226
089	768	965	376	982	244
141	809	992	395	1,012	260
186	843	1,049	431	042	276
		1,111	1,463	1,074	1,290
		138	474	108	303
				128	309

TABLE VII

M_∞	3,0	4,0	5,0
θ_{2s}	0,946	0,921	0,905
θ_{sep}	0,959	0,892	0,865

DISTRIBUTION

Addressee	Copy No.
AFBMD, Attn: WDSOT (+ 1 Reproducible)	1-33
ARL, Attn: M. Adams	34
ARL, Attn: Technical Library	35
Aeronutronic Systems, Inc., Attn: J. V. Charyk	36
Bell Aircraft Corp., Attn: W. Squire	37
Bendix Aviation Corp., Attn: E. W. Lewis	38
Brooklyn Polytechnic Institute, Attn: M. Bloom	39
Brooklyn Polytechnic Institute, Attn: P. Libby	40
Brooklyn Polytechnic Institute, Attn: A. Ferri	41
Brooklyn Polytechnic Institute, Attn: F. Pohle	42
Brown University, Attn: M. Holt	43-52
Brown University, Attn: R. Probstein	53
California Institute of Technology, Attn: F. Goddard	54
California Institute of Technology, Attn: L. Lees	55
California Institute of Technology, Attn: H. W. Liepmann	56
Convair Aircraft Corp., Attn: W. H. Patterson	57
Cornell Aeronautical Laboratory, Attn: A. Flax	58
Cornell University, Attn: E. L. Resler	59
Douglas Aircraft Co., Attn: H. Luskin	60
Douglas Aircraft Co., Attn: R. L. Johnson	61
General Electric Co., (MOSD), Attn: F. Gravallos	62
Harvard University, Attn: G. Carrier	63
Harvard University, Attn: H. W. Emmons	64
Hughes Aircraft Co., Attn: A. Puckett	65
Institute of Aeronautical Sciences, Attn: Aeronautical Engineering Review	66
Johns Hopkins University, Attn: S. Corrsin	67
Lockheed Aircraft Corp., Attn: G. H. Backer	68
Lockheed Aircraft Corp., Attn: M. Tucker	69
Martin Co., Attn: E. E. Clark	70
Martin Co., Attn: S. C. Traugott	71
Massachusetts Institute of Technology, Attn: J. Baron	72
Massachusetts Institute of Technology, Attn: M. Finston	73
Massachusetts Institute of Technology, Attn: C. C. Lin	74
Massachusetts Institute of Technology, Attn: L. Trilling	75
NACA, Langley Field, Attn: A. Busemann	76
NACA, Langley Field, Attn: M. Cooper	77
NACA, Langley Field, Attn: S. Katzoff	78
NACA, Moffett Field, Attn: H. J. Allen	79
New York University, Attn: J. B. Keller	80
New York University, Attn: J. F. Ludloff	81
North American Aviation, Inc., Attn: E. R. Van Driest	82

DISTRIBUTION (Cont'd)

Addressee	Copy No.
Office of Scientific Research, Western Div., Attn: M. Alperin	83
Princeton University, Attn: S. I. Cheng	84
Princeton University, Attn: L. Crocco	85
Rand Corp., Attn: C. Gazley	86
RCA, Burlington,Mass., Attn: R. Fleddermann	87
Rensselaer Polytechnic Institute, Attn: T. Y. Li	88
Republic Aviation Corp., Attn: R. J. Sanator	89
Southwest Research Institute, Attn: Applied Mechanics Review	90
STL, Attn: R. Bromberg	91
STL, Attn: M. U. Clauser	92
STL, Attn: C. B. Cohen	93
United Aircraft Corp., Attn: J. G. Lee	94
University of Maryland, Attn: S. I. Pai	95
University of Michigan, Attn: A. M. Kuethe	96
University of Minnesota, Attn: E. R. Eckert	97
U.S. Naval Ordnance Laboratory, Attn: Z. I. Slawsky	98
W. Bade	99
C. Berninger	100
W. B. Brower	101
F. W. Diederich	102
S. Globe	103
R. John	104
A. Kahane	105
M. Klamkin	106
J. Klugemann	107
P. Levine	108
E. Migotsky	109
E. Offenharts	110
W. Stephenson	111
D. R. Walker	112
J. Warga	113
M. Zlotnick	114-123
Yellow File	124
Aerodynamic Files	125-129
Central Files	130
Document Control	131-135
Research Library	136, 137